JOURNAL OF GEOPHYSICAL RESEARCH, VOL. 112, D14103, doi:10.1029/2006JD008231, 2007

Interannual variation in biogenic emissions on a regional scale

Lindsey E. Gulden,[1] Zong-Liang Yang,[1] and Guo-Yue Niu[1]

Received 7 November 2006; revised 19 February 2007; accepted 4 May 2007; published 21 July 2007.

[1] Interannual variation in biogenic emissions is not well quantified, especially on regional scales. We use a land surface model augmented with a short-term dynamic phenology scheme to estimate the interannual variation in the emission of biogenic volatile organic compounds (BVOCs) between 1982 and 2004. We use North American Regional Reanalysis data to drive two versions of the National Center for Atmospheric Research Community Land Model (CLM) on a 0.1° grid over eastern Texas. The first version is the standard CLM with prescribed leaf area index (LAI) (i.e., LAI varies seasonally but not interannually); the second version is the standard CLM augmented with a dynamic phenology scheme (CLM-DP) that allows LAI to respond to environmental variation. We calibrate CLM-DP using satellite-derived LAI as our visual constraint. When phenology is prescribed, the domain-mean (domain-maximum) average absolute departure from the monthly mean BVOC flux is 11.7% (70.6%); when phenology is allowed to vary with environmental conditions, it is 22.4% (137.7%). The domain-mean (domain-maximum) average absolute departure from the monthly mean flux is lower during summer: using CLM-DP, it is 15.7% (35.3%); using the standard CLM, it is 7.0% (23.0%). The domain-average, mean-normalized standard deviation of the June-July-August mean BVOC flux is 0.0619 when LAI is prescribed and 0.183 when LAI varies with environmental conditions. Our results imply that interannual variation of leaf biomass density, which is primarily driven by interannual variability of precipitation, is a significant contributor to year-to-year differences in BVOC flux on a regional scale, of at least equal importance to interannual variation of temperature and shortwave radiation. Phenology-driven biogenic emission variability is most pronounced in regions with relatively low emissions: as a grid cell's mean BVOC flux decreases, the mean-normalized standard deviation of BVOC flux tends to increase. BVOC flux is most variable between years in subhumid, sparsely wooded regions where interannual variability of precipitation is relatively large.

Citation: Gulden, L. E., Z.-L. Yang, and G.-Y. Niu (2007), Interannual variation in biogenic emissions on a regional scale, *J. Geophys. Res.*, *112*, D14103, doi:10.1029/2006JD008231.

1. Introduction

[2] Biogenic volatile organic compounds (BVOCs) are involved in a suite of environmental processes. BVOCs condense to form secondary organic aerosols [*Kavouras et al.*, 1998; *Claeys et al.*, 2004], which often become cloud condensation nuclei [*Novakov and Penner*, 1993] and which alter the radiative balance at Earth's surface [*Andreae and Crutzen*, 1997]. BVOCs react in the presence of nitrogen oxides to increase the concentration of tropospheric ozone, which is a respiratory irritant and a primary constituent of photochemical smog [*Chameides et al.*, 1988]. High concentrations of ozone adversely affect plant photosynthesis and growth [*Ashmore*, 2005]. The ultimate reaction product of most BVOCs is carbon dioxide [*Guenther*, 2002], and the presence of isoprene may increase the lifetime of methane [*Poisson et al.*, 2000], a potent greenhouse gas. Because a diverse set of environmental processes responds to forcing by biogenic emissions, year-to-year variation in the flux of BVOCs has the potential to influence interannual climate variability.

[3] A range of factors affect the rate of biogenic emissions. The vegetation species composition of a landscape, which is controlled in large part by local climate, exerts primary control on the flux of BVOCs from the land surface. The rate of biogenic emissions also has been shown to vary as a function of leaf biomass density, the amount of photosynthetically active radiation (PAR) reaching the leaf surface, the canopy temperature, leaf age [*Guenther et al.*, 1991; *Monson et al.*, 1994; *Fuentes et al.*, 1995], soil nutrient availability, ambient carbon dioxide concentration [*Possell et al.*, 2004], drought stress, and the leaf-to-air vapor-pressure deficit [*Pegoraro et al.*, 2005]. Multiple researchers have examined factors controlling seasonal variation in biogenic emissions [e.g., *Monson et al.*, 1994; *Fuentes and Wang*, 1999]. Here we focus on interannual variation.

[1]Department of Geological Sciences, John A. and Katherine G. Jackson School of Geosciences, University of Texas at Austin, Austin, Texas, USA.

0148-0227/07/2006JD008231$09.00

[4] Year-to-year variation in BVOC flux is likely considerable. *Levis et al.* [2003] used a biogenic emissions module [*Guenther et al.*, 1995] and a dynamic global vegetation module (DGVM) within a climate model to show that the interannual variation in the total global flux of BVOCs in a given month exceeded 18% during a 10-year fully coupled climate simulation. *Naik et al.* [2004] drove the Integrated Biosphere Simulator (IBIS), a DGVM, from 1971–1990 and found that modeled seasonal variability of total global biogenic emissions ranged from 17–25%. *Tao and Jain* [2005] used a terrestrial biosphere model to represent 1981–2000 and found that, when they represented both carbon dioxide fertilization of the biosphere and monthly-scale climate variability, global total isoprene emissions for a given month varied up to 31% between years. These estimates of interannual variation in monthly BVOC flux are lower than the satellite-derived estimate of 40% provided by *Palmer et al.* [2006], who used a combination of six years of satellite observations (40 km × 320 km) and model simulations (2° × 2.5°) to estimate the interannual variability of isoprene emissions in the southeastern United States. Presumably, interannual variation in biogenic emissions on a regional scale is larger than that on a global scale, where estimates are effectively smoothed by averaging across all land.

[5] Less attention has been paid to providing high-resolution, regional-scale assessments of biogenic emissions variability. The effects of BVOCs and their reaction products on cloud formation and atmospheric radiative transfer make them an important constituent to represent within future generations of regional climate models. Regional-scale climate impact assessments are of value to policy-makers (e.g., air quality managers, urban planners), who design regulations and resource management plans for localities and regions.

[6] Regardless of the size of the modeling domain, most efforts to model BVOC emissions employ the empirical algorithm of *Guenther et al.* [1995], which simulates emission of isoprene (the most dominant BVOC species), monoterpene, other volatile organic compounds (VOCs), other reactive VOCs, and carbon monoxide (which it treats as if it were emitted from vegetation). The 1995 Guenther algorithm represents BVOC flux as a function only of plant species, PAR, canopy temperature, and leaf biomass density:

$$F_{BVOC} = \varepsilon \gamma_{PAR} \gamma_T D \quad (1)$$

where F_{BVOC} is the land surface-to-atmosphere flux of BVOCs (units: μg C m^{-2} h^{-1}); ε is a vegetation-type-specific emission capacity (units: μg C $gdlm^{-1}$ h^{-1}, where gdlm is g dry leaf matter); γ_{PAR} is a dimensionless scalar that is a nonlinear function of PAR reaching the canopy surface (for nonisoprene BVOCs, $\gamma_{PAR} = 1$); γ_T is a dimensionless scalar that adjusts BVOC flux in response to changes in canopy temperature; and D is the leaf biomass density (units: g dry leaf matter [gdlm] m^{-2} of ground covered by the vegetation type). More recent modifications to the algorithm consider seasonal variation in plant emitting capacities and explicitly account for variation in soil moisture as a source of variability in BVOC emission rates [*Guenther et al.*, 2006]. For the research presented here, we assume that the *Guenther et al.* [1995] algorithm captures the key environmental drivers of emission variability.

[7] Even if the *Guenther et al.* [1995] algorithm is assumed to perfectly represent the emissions processes, realistic simulation of BVOC flux also requires accurate representation of each of the three component sources of variation in the *Guenther et al.* [1995] algorithm: (1) short-term environmental variation (i.e., PAR reaching the leaf surface and canopy temperature); (2) seasonal and interannual changes in leaf biomass density (phenology), which vary with changing environmental conditions (e.g., spring soil temperatures, plant-available soil moisture in the early summer); and (3) the species composition of a landscape.

[8] Previous researchers' model-derived estimates of BVOC flux variability lay the foundation for future work [*Levis et al.*, 2003; *Naik et al.*, 2004; *Tao and Jain*, 2005], but their model frameworks do not realistically represent all three component sources of variation listed above. *Naik et al.* [2004] and *Tao and Jain* [2005] used monthly mean climate data to drive their models. Because biogenic emissions are a highly nonlinear function of PAR and canopy temperature, use of monthly mean climate data to drive a model likely underestimates total emissions and the variability of emissions. *Naik et al.* [2004] and *Levis et al.* [2003] used dynamic global vegetation models (DGVMs) to represent interannual phenological variation. The rate at which most species of trees emit biogenic emissions is one to two orders of magnitude higher than the rate at which grasses emit BVOCs. Accurate specification of the tree-to-grass ratio on the model domain landscape is consequently of critical importance when modeling biogenic emissions, but the skill of DGVMs to reproduce vegetation type composition at high resolutions has not been demonstrated. For example, the DGVM used by *Levis et al.* [2003] overestimates the ratio of grass to trees, most likely because of a dry bias in the coupled land surface model (LSM) soil profile [*Bonan and Levis*, 2006]. Furthermore, DGVMs may not accurately represent vegetation dynamics, phenology, or carbon and water fluxes at high model resolutions [*Kucharik et al.*, 2006].

[9] When designing the model framework for the research described here, we sought to use the most realistic currently available representations of the processes to which biogenic emissions estimates are most sensitive on timescales of years to decades (i.e., meteorological variation, seasonal and interannual variation in leaf biomass density, vegetation composition of the model landscape). We employed a process-based, short-term dynamic phenology module within the National Center for Atmospheric Research's Community Land Model (CLM) [*Bonan et al.*, 2002a, 2002b; *Levis et al.*, 2004; *Oleson et al.*, 2004, available at http://www.cgd.ucar.edu/tss/clm/distribution/clm3.0/TechNote/CLM_Tech_Note.pdf], a current-generation land surface model (LSM) that contains a biogenic emissions module [*Levis et al.*, 2003]. LSMs allow biomass density, PAR, and canopy temperature to vary within a physically consistent framework and can be used for both retrospective analysis and predictive research. *Gulden and Yang* [2006] showed that when equipped with species-based regional emissions capacities for LSM land cover types, regional LSMs adequately reproduce the spatial distribution and magnitude of BVOC flux when compared to species-

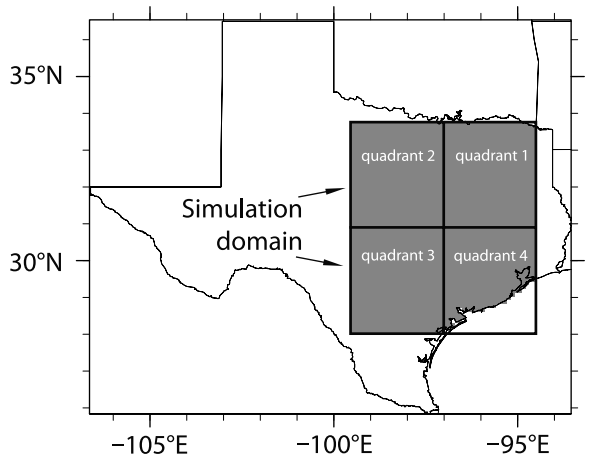

Figure 1. Model domain. Quadrant-mean LAI values were used as an additional visual constraint when calibrating the dynamic phenology module within CLM (see description of calibration in text).

based emissions modules. Our framework realistically represents meteorological forcing, updating model state variables with new meteorological input every hour. After preliminary model calibration, the simulated phenology is consistent with observed phenological variation. The species distribution of the model landscape is also realistic: to initialize the model, we used land cover data and biogenic emissions factors that were derived from the same high-resolution, ground-survey-derived, species-based land cover data set [*Wiedinmyer et al.*, 2001; *Gulden and Yang*, 2006]. Although climate-driven vegetation composition change over many centuries can result in a several-fold change in biogenic emissions [*Lathière et al.*, 2005], we assume that over the course of years to decades, the relative plant-type distribution of a landscape can be considered effectively constant.

[10] We use the augmented CLM (as described above) to address the following questions: (1) On a regional scale, how much do biogenic emissions for a given month vary from year to year? (2) Approximately what portion of this variation is due to direct climate variation (e.g., changes in PAR reaching the canopy, changes in leaf surface temperature)? (3) Approximately what portion of this variation can be attributed to interannual changes in the amount of leaf biomass resulting from short-term variation in environmental conditions (e.g., more rain, warmer spring temperatures)? We present a model framework that can be used to represent the response of biogenic emissions to changing climate conditions on a regional scale. Our method is demonstrated for eastern Texas, but it can be readily applied elsewhere.

2. Models and Methods

[11] We coupled a short-term dynamic phenology model [*Dickinson et al.*, 1998] to CLM and used the biogenic emissions module added by *Levis et al.* [2003] (see equation (1)) [*Guenther et al.*, 1995]. Estimates of total BVOCs emitted globally using CLM with Levis et al.'s BVOC emissions module are consistent with numerous other estimates [e.g., *Guenther et al.*, 1995; *Wang and Shallcross*, 2000].

[12] We simulated biogenic emissions on a 0.1° grid over eastern Texas (28°N to 33.5°N; −99.5°E to −94.5°E) (Figure 1) using a 10-km, species-based land cover data set [*Gulden and Yang*, 2006]. Vegetation composition varies considerably across the domain: a mixed broadleaf and needleleaf evergreen forest covers far eastern Texas; a mosaic of woody savannas, grassland, and cropland covers the rest of the domain. There is a strong west–east gradient in mean annual precipitation (Figure 2), which is reflected in the prominent west–east gradient in biomass density (Figure 3).

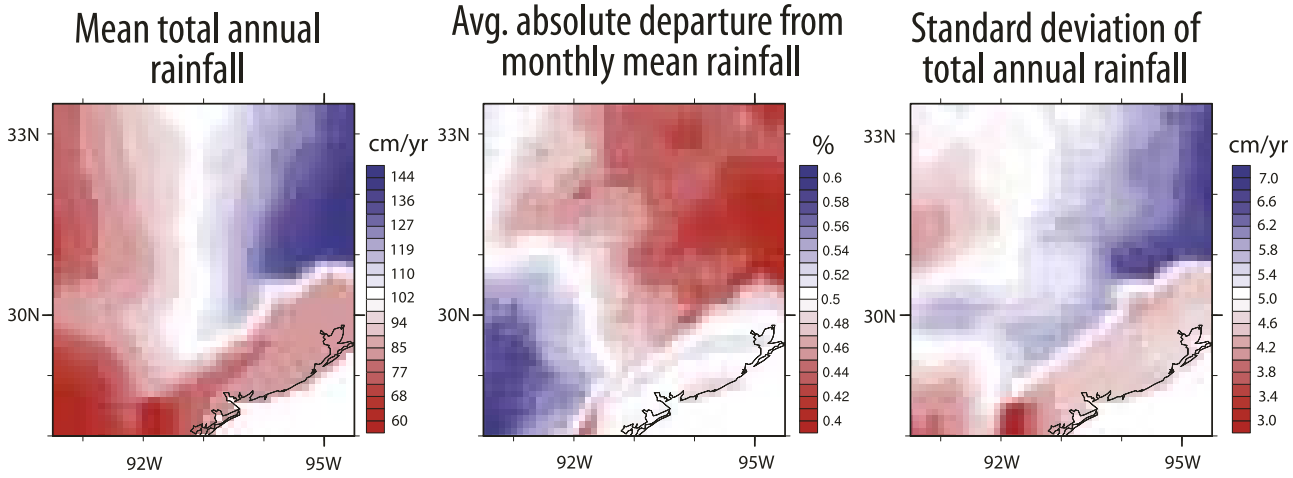

Figure 2. Annual rainfall characteristics of meteorological forcing used to drive model. Data are bilinearly interpolated to 0.1° from North American Regional Reanalysis (NARR) data [*Mesinger et al.*, 2006] for years 1982–2004. Note the dry bias of the NARR data along coastal Texas; resulting LAI values simulated with the dynamic phenology module are correspondingly spuriously small.

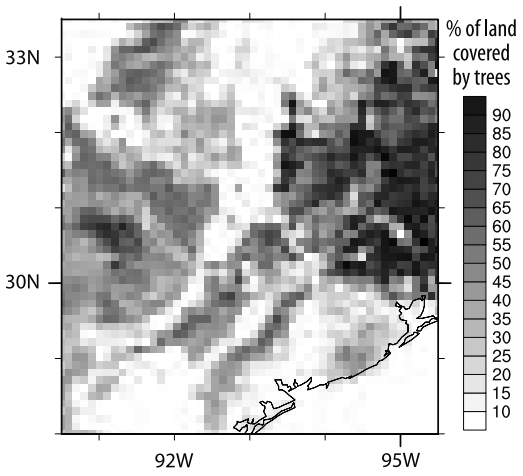

Figure 3. Percent of land area covered by trees. Data shown were derived from the ground-survey-derived, vegetation-species-based land cover data set of *Wiedinmyer et al.* [2001] by *Gulden and Yang* [2006].

2.1. Community Land Model

[13] CLM is representative of a current-generation LSM used in climate and weather research. It simulates the flow of mass, energy, and momentum between different reservoirs of the land surface. CLM represents canopy radiative transfer [*Dickinson*, 1983; *Sellers*, 1985; *Bonan*, 1996], photosynthesis and stomatal conductance [*Farquhar et al.*, 1980; *Collatz et al.*, 1991, 1992; *Dougherty et al.*, 1994], and transpiration [*Oleson et al.*, 2004, available at http://www.cgd.ucar.edu/tss/clm/distribution/clm3.0/TechNote/CLM_Tech_Note.pdf]. CLM can be driven as part of a fully coupled climate system model or "offline" using preexisting, high-resolution meteorological forcing data. Model time steps are short (minutes to hours).

2.2. Dynamic Phenology Module

[14] So that we could still simulate interannual variation in leaf biomass density without having our model results depend on CLM-DGVM's spuriously high ratio of grass to trees [*Bonan and Levis*, 2006], we replaced CLM's DGVM with a dynamic phenology module [*Dickinson et al.*, 1998]. Unlike CLM-DGVM, the augmented LSM (CLM-DP) keeps the plant functional type (PFT) fraction of a grid cell equal to that specified at model initialization, but it allows leaf biomass density to vary as a function of soil moisture, soil temperature, canopy temperature, and vegetation type.

[15] The dynamic phenology module allocates carbon assimilated during photosynthesis to leaves, roots, and stems; the fraction of photosynthate allocated to each reservoir is a function of the existing LAI. LAI is a linear function of leaf biomass density of the landscape; we used PFT-specific leaf biomass densities derived in concert with the initialization data set [*Gulden and Yang*, 2006]. The model tracks growth and maintenance respiration, represents slow-turnover and fast-turnover carbon reservoirs, and simulates vegetation response to cold stress and drought stress. Because the dynamic phenology module represents LAI as a nonlinear function of multiple environmental variables, the relationship between climate and LAI is not straightforward: in general, wetter soil, higher rates of photosynthesis, warm soil, and temperate canopy air result in increased LAI. *Dickinson et al.* [1998] provides a detailed description of the model.

[16] The adequacy of the *Dickinson et al.* [1998] or an equivalent dynamic phenology model to realistically represent changes in leaf biomass is not well established [*Kim and Wang*, 2005]. Our review of the ecological literature leads us to believe that there is not yet firm consensus in the ecological research community regarding the quantification of factors that control short-term variation in biomass [e.g., *Grier and Running*, 1977; *Gholz*, 1982; *Leuschner et al.*, 2006]. The *Dickinson et al.* [1998] scheme was based on the best available understanding of carbon allocation between vegetation reservoirs and is therefore a reasonable choice for representing short-term phenological variation. The *Dickinson et al.* [1998] model does not represent long-term competition between vegetation types and is not susceptible to model-produced errors in vegetation-type distribution, which pose a potentially significant source of error for biogenic emissions estimates.

2.3. Modifications to Model Processes and Parameters

[17] So that timing and shape of the seasonal cycle of the dynamically simulated LAI would better match those of the satellite-observed LAI, we changed the shape of the function allocating assimilated carbon to leaves (Figure 4) and recoded the model so that leaves receive no assimilated carbon outside of the model growing season. Our selection of carbon allocation function was guided by the function's influence on the shape of the seasonal cycle of the modeled LAI. Following CLM-DGVM, we treated the stem area index (SAI) as a constant fraction of LAI. SAI represents nonwoody, nonleaf biomass above ground; as SAI increases, the shaded fraction of the canopy also increases.

[18] To ensure that modeled seasonal cycle and magnitude of seasonal variation in LAI were consistent with observations, we manually calibrated the parameters of CLM-DP. We used two satellite-derived monthly time series

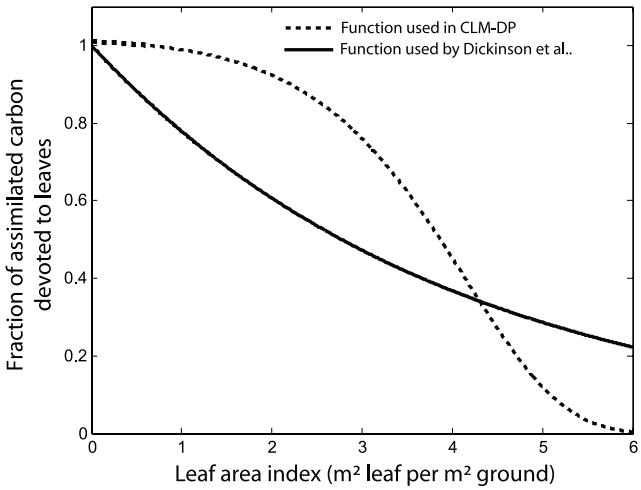

Figure 4. Fraction of assimilated carbon devoted to leaves as a function of leaf area index. Comparison of the original function used by *Dickinson et al.* [1998] with that used in CLM-DP.

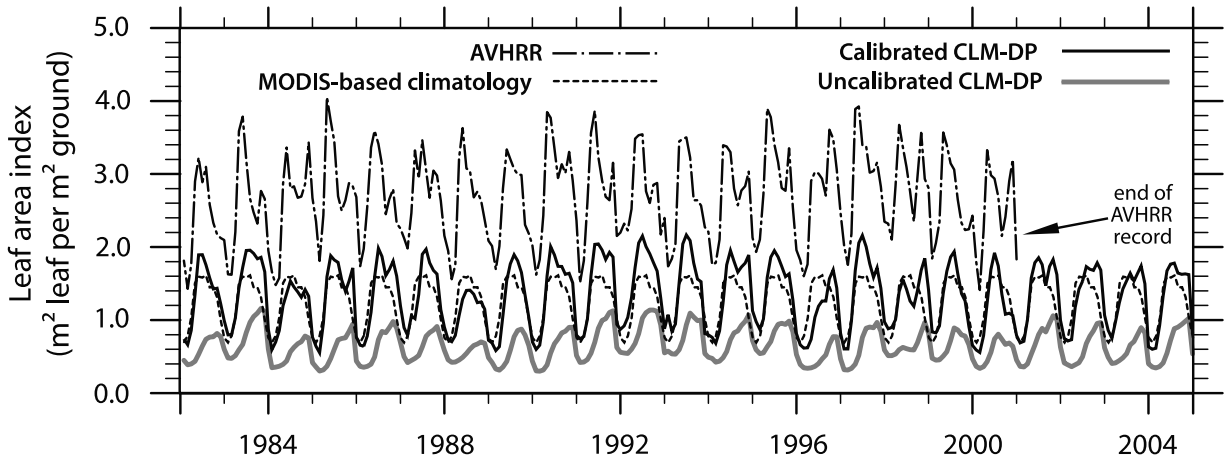

Figure 5. Comparison observed and simulated domain-average monthly leaf area index (LAI) for 1982–2004. The MODIS-based climatology varies seasonally but not interannually. The "Calibrated CLM-DP" series is the LAI simulated by CLM-DP after manual calibration to the satellite-derived LAI and our modifications to the code (both of which are described in text). The "Uncalibrated CLM-DP" series is the LAI simulated by CLM-DP without any modifications to the parameterizations or the parameters.

as visual constraints (Figure 5): (1) the domain-averaged LAI for 1982–2000, which we calculated from 0.5° × 0.5° Advanced Very High Resolution Radiometer (AVHRR) data and (2) the domain-averaged climatological LAI (i.e., the mean annual cycle averaged from data spanning 2001–2003) obtained from Moderate Resolution Imaging Spectroradiometer (MODIS) and AVHRR data [*Lawrence and Chase*, 2007].

[19] The MODIS climatological LAI provides no information about interannual variability. AVHRR LAI data for 1982–2000 provided us with a lengthy, continuously varying time series. However, AVHRR-derived LAI data likely overestimates the magnitude of the mean LAI in eastern Texas [*Tian et al.*, 2004; *Lawrence and Chase*, 2007] and underestimates interannual variation in LAI because it is based on the Normalized Difference Vegetation Index, which saturates quickly, especially in forested regions such as eastern Texas [e.g., *Wang et al.*, 2005]. We used the MODIS climatological LAI time series as the target for the mean magnitude and amplitude of the seasonal cycle; we used the AVHRR LAI data to inform our understanding of the variability of LAI in the model domain.

[20] We adjusted parameters until the shape of the seasonal cycle of LAI and the timing of leaf-on and leaf-off roughly matched the satellite-derived data. We uniformly scaled the specific leaf area values for PFTs calculated by *Gulden and Yang* [2006] by 1.5. For each PFT, we increased the minimum LAI from 0.05 m^2 m^{-2} to one half of the domain-wide minimum values reported in the MODIS-derived land cover data set [*Lawrence and Chase*, 2007]. For woody vegetation, we set SAI equal to 0.25 × LAI; for grasses, we set SAI equal to 0.05 × LAI. CLM uses SAI to calculate the shaded fraction of the canopy; the dependence of the rate of photosynthesis on the shaded fraction makes the modeled LAI particularly sensitive to the SAI fraction. Other slight adjustments to parameters were used if they improved the visual match of the data sets to the satellite-derived data; however, model output was insensitive to most parameters.

[21] Figure 5 shows observed, uncalibrated, and calibrated domain-average LAI. The average absolute percent departure from the mean LAI (see Appendix A for definition) provides a measure of variability that is not directly tied to the magnitude of LAI. Table 1 provides the average and maximum absolute percent deviation from the monthly mean domain-average LAI. Calibration of the dynamic phenology module decreased the average absolute percent deviation from the monthly mean LAI from 15.2% to 12.9%, which made the variability of the simulated LAI more consistent with that of the AVHRR data set. Manual calibration improved simulated LAI across the domain: the calibrated, quadrant-averaged LAI for each of the four quadrants of the domain (see Figure 1) is consistent with

Table 1. Observed and Model-Simulated Leaf Area Index (LAI): Average and Maximum Absolute Percent Departure From the Domain-Averaged Monthly Mean[a]

	Whole Domain	Quadrant 1	Quadrant 2	Quadrant 3	Quadrant 4
AVHRR[b]					
Average	9.0%	6.1%	15.0%	18.0%	8.7%
Maximum	30.7%	29.3%	68.1%	109.4%	30.4%
Uncalibrated CLM-DP					
Average	15.2%	9.3%	10.4%	23.3%	29.3%
Maximum	49.6%	57.9%	49.4%	90.8%	90.2%
Calibrated CLM-DP					
Average	12.9%	9.7%	11.4%	18.4%	22.9%
Maximum	59.3%	62.8%	61.3%	78.3%	59.9%

[a]The average and maximum absolute percent departure from the monthly mean is defined in Appendix A.

[b]The AVHRR LAI series, which is on a 0.5° grid, extends only from 1982–2000; the model_simulated LAI series, which are simulated on a 0.1° grid, extend from 1982–2004.

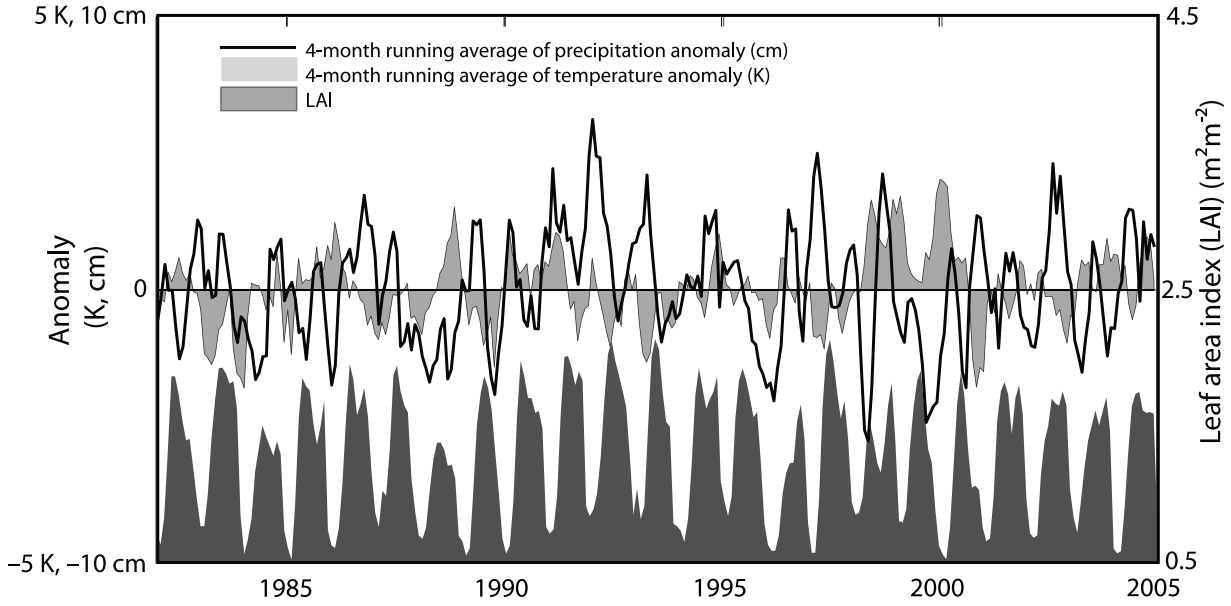

Figure 6. Domain-averaged temperature anomaly, precipitation anomaly, and leaf area index (LAI). Temperature and precipitation anomalies were derived from the North American Regional Reanalysis (NARR) data [*Mesinger et al.*, 2006] used to drive the offline models.

the quadrant-averaged satellite observations (data not shown). Anomalies of the calibrated LAI are consistent in both sign and magnitude with those of the satellite-derived data (results not shown).

[22] Figure 6 shows the relationship between CLM-DP-simulated LAI and domain-average precipitation and temperature anomalies. As expected, LAI is lowest in hot, dry years and highest in wet, temperate years. Year-to-year differences in precipitation appear more important in determining LAI variation than do year-to-year differences in temperature.

2.4. Model Runs

[23] We report the results of two model runs: (1) One run used the standard version of CLM (CLM-PRESC); it prescribed the MODIS climatological LAI for each model year. (2) The second run used CLM-DP; it simulated LAI variation in response to changing meteorological conditions. For both runs, we specified the plant functional type (PFT) composition of the landscape using a 0.1°, land cover data set that *Gulden and Yang* [2006] derived from a 1-km species-based data set that was compiled from extensive ground surveys [*Wiedinmyer et al.*, 2001]. *Gulden and Yang* [2006] used the species-based data set to calculate species-based, region-specific biogenic emissions factors for each PFT (ε in equation (1)), which we used in both runs.

[24] Bilinearly interpolated North American Regional Reanalysis (NARR) data [*Mesinger et al.*, 2006] provided 0.1° meteorological forcing. We simulated the period 1979–2004, using a 1-hour model time step. Simulation years 1979–1981 served as the spin-up period. We analyzed monthly mean model output from model years 1982–2004. The meteorological forcing was the same for both runs.

3. Results and Discussion

[25] A time series of simulated domain-mean BVOC flux is shown in Figure 7. Because the uncertainty in the magnitude of BVOC emissions probably exceeds a full order of magnitude [e.g., *Guenther*, 1997; *Simpson et al.*, 1999; *Smiatek and Bogacki*, 2005], we report simulated variability using the average absolute percent departure from the monthly mean, a measure of variability that is

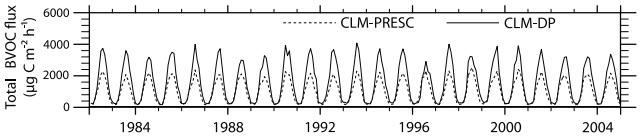

Figure 7. Time series of domain-averaged BVOC flux. BVOC flux is the sum of the fluxes of isoprene, monoterpene, other reactive volatile organic compounds, other volatile organic compounds, and carbon monoxide (which CLM treats as if it were emitted by vegetation). Although both the CLM-PRESC and CLM-DP runs used the same ground-survey-based PFT distribution, CLM-PRESC relied on PFT-specific LAI values obtained from the MODIS-derived land cover data set [*Lawrence and Chase*, 2007]. The ground-survey-based data set has, on average, a higher area fraction of bare soil than the *Lawrence and Chase* [2007] data set; consequently, CLM-PRESC mean LAI is smaller than the MODIS climatological observations. The magnitude of the BVOC flux simulated using CLM-PRESC is correspondingly lower.

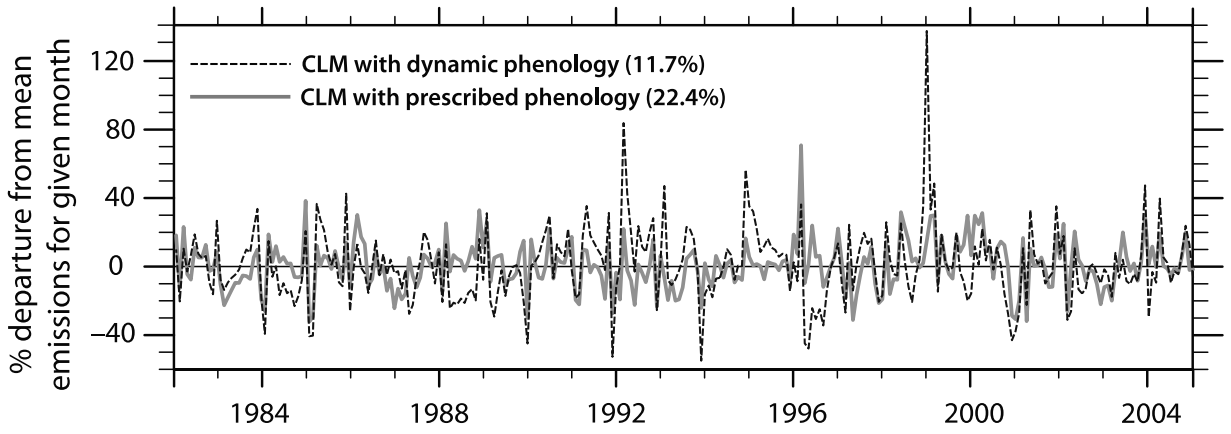

Figure 8. Percent departure from the monthly mean BVOC emissions. Average absolute percent departure from the monthly mean is in parentheses. BVOC flux is the sum of the fluxes of isoprene, monoterpene, other volatile organic compounds, other reactive volatile organic compounds, and carbon monoxide (which CLM treats as if it were emitted by vegetation). See Appendix A for definition of average absolute percent departure from the monthly mean.

not directly tied to the magnitude of the simulated flux (see definition in Appendix A). To provide information about absolute flux, we also report the standard deviation and its mean-normalized counterpart, the coefficient of variation (CV).

[26] The domain-mean average absolute departure from the monthly mean BVOC flux was 22.4% when we used CLM-DP and 11.7% when we used CLM-PRESC (Figure 8 and Table 2); the domain-maximum average absolute departure from the monthly mean BVOC flux increased from 70.6% (using CLM-PRESC) to 137.7% (using CLM-DP) (Table 2). When only the BVOC fluxes from June, July, and August (JJA) were considered, the domain-mean (domain-maximum) average absolute departure from the monthly mean BVOC flux fell to 15.7% (35.3%) when we employed CLM-DP and to 7.0% (23.0%) when we used CLM-PRESC. A similar decrease was observed in each of the four quadrants (Figure 1) of the domain (results not shown).

[27] We present detailed results for JJA because biogenic emissions peak in the summer months, concurrent with the summer ozone season in Texas. This is the time period when the biogenic emissions may play the most important role in the regional atmospheric chemistry. It is important to note that some BVOC-related climatic processes may be most sensitive to relative variability during other seasons; however, because such processes are poorly understood, we focus on the period of the year when absolute BVOC flux is greatest.

[28] Leaf biomass density variation is a significant source of interannual variation in JJA mean BVOC flux: the domain-average standard deviation of the seasonal (JJA) mean BVOC flux for the period 1982–2004 is 123 μg C m^{-2} h^{-1} when phenology is prescribed and 401 μg C m^{-2} h^{-1} when phenology is allowed to vary with environmental conditions. Use of dynamic phenology results in threefold increase in the domain-average CV of JJA mean BVOC flux: the CV is 0.183 when CLM-DP is used and 0.0619 when CLM-PRESC is used.

[29] Figures 9a and Figure 9d show the spatial distribution of the simulation mean JJA BVOC flux. Model results are qualitatively consistent with expectations: biogenic emissions peak in the evergreen-deciduous mixed forests of eastern Texas, where biomass density is highest and where the dominant vegetation species have high emission capacities. Figures 9b and Figure 9e show the spatial distribution of the average absolute departure from the JJA mean flux; Figures 9c and Figure 9f show the spatial distribution of the standard deviation of the JJA mean flux.

Table 2. VOC Flux Simulated Using Prescribed Phenology and Dynamic Phenology: Average and Maximum Absolute Percent Departure From Monthly Mean BVOC Flux[a]

	Whole Domain	Quadrant 1	Quadrant 2	Quadrant 3	Quadrant 4
			Total[b] *BVOC Flux*		
Prescribed phenology					
Average	11.7%	1.32%	13.5%	12.6%	7.3%
Maximum	70.6%	74.9%	105.6%	78.9%	26.4%
Dynamic phenology					
Average	22.4%	20.9%	19.4%	27.6%	21.7%
Maximum	137.7%	225.1%	159.9%	129.1%	70.7%
			Isoprene		
Prescribed phenology					
Average	12.7%	14.8%	13.2%	13.2%	8.2%
Maximum	89.3%	97.7%	139.4%	91.1%	29.6%
Dynamic phenology					
Average	25.5%	25.0%	24.1%	30.6%	22.4%
Maximum	203.7%	331.4%	288.0%	150.2%	80.6%
			Monoterpene		
Prescribed phenology					
Average	9.9%	10.5%	12.4%	11.1%	5.3%
Maximum	42.3%	49.9%	67.9%	54.5%	21.1%
Dynamic phenology					
Average	19.2%	15.9%	16.0%	25.2%	19.9%
Maximum	79.0%	120.2%	80.7%	91.6%	50.9%

[a]See Appendix A for explanation of average and maximum absolute departure from the monthly mean.

[b]Total VOC flux is the sum of the fluxes of isoprene, monoterpene, other volatile organic compounds, other reactive volatile organic compounds, and carbon monoxide (which CLM treats as if it were emitted by vegetation).

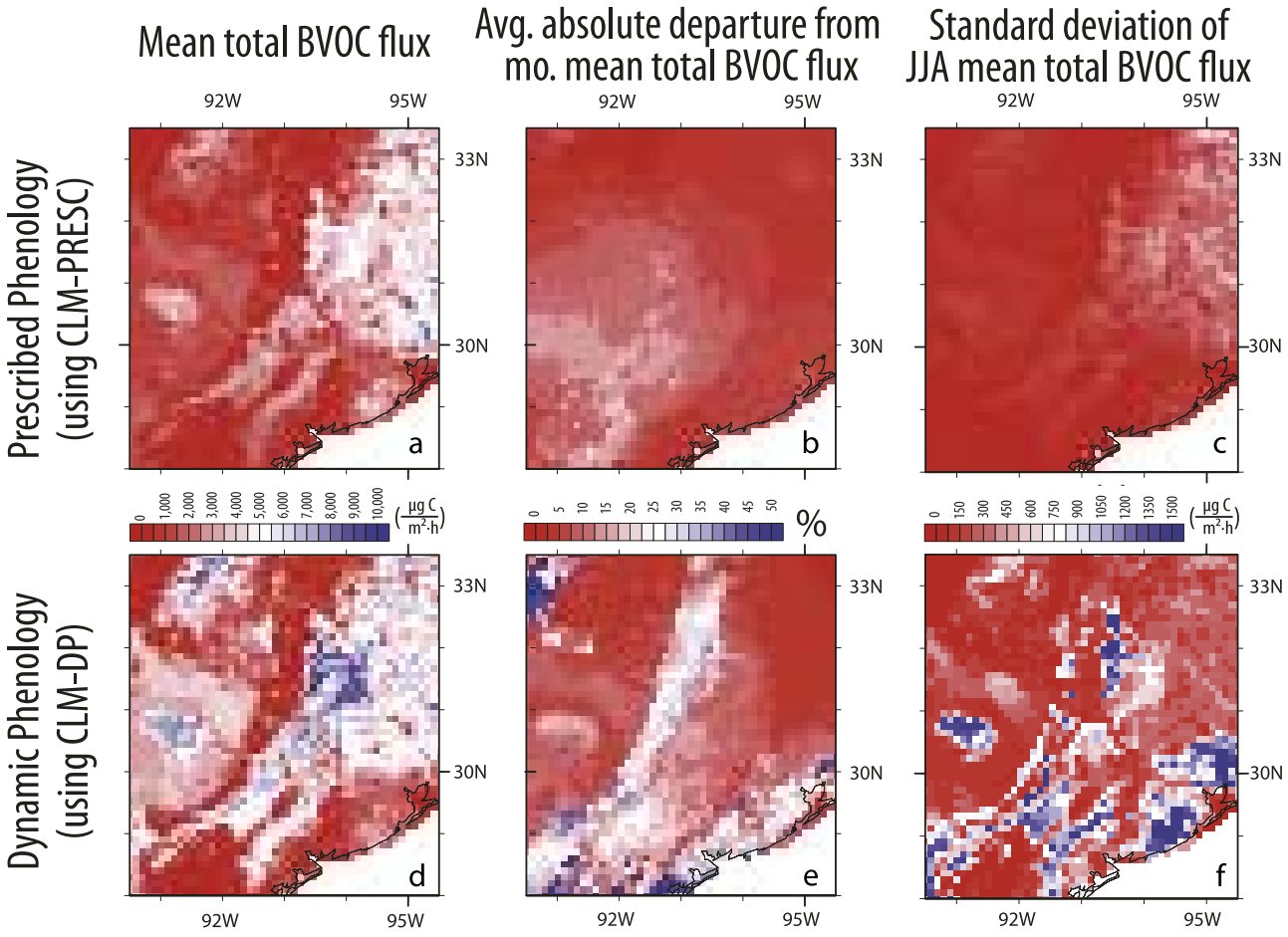

Figure 9. Summer BVOC flux (1982–2004). (a–c) Results for prescribed phenology runs and (d–f) results when dynamic phenology is employed. Figures 9a and 9d show the mean total BVOC flux, Figures 9b and 9e show the average absolute departure from the monthly mean total BVOC flux, and Figures 9c and 9f map the standard deviation of JJA monthly total BVOC flux. The standard deviation quantifies the interannual variation in the mean seasonal (mean of June, July, and August emissions) average BVOC flux. BVOC flux is the sum of the fluxes of isoprene, monoterpene, other reactive volatile organic compounds, other volatile organic compounds, and carbon monoxide. Appendix A explains the calculation of the average absolute departure from the monthly mean.

Grid cells where variability is largest are often grid cells in which there are relatively few trees (e.g., in the northwest corner of the domain) (Figure 3) and where annual precipitation is relatively low but also highly variable between years (Figure 2). It logically follows that interannual variation in BVOC flux is highest in areas where the absolute BVOC flux is relatively low: as the JJA mean BVOC flux increases, the grid cell's CV of JJA mean BVOC flux becomes less sensitive to interannual variation in LAI (Figure 10).

[30] Modeled isoprene emissions are more sensitive than modeled monoterpene emissions to use of dynamic phenology (Table 2). Modeled isoprene flux is a nonlinear function of both PAR and canopy temperature (both of which are altered by changing LAI), whereas monoterpene flux responds only to changes in canopy temperature.

[31] Even though BVOC flux is a linear function of biomass density (equation (1)), there is not a one-to-one correspondence between the CV of the JJA mean LAI and the CV of the JJA mean BVOC flux (Figure 11). LAI nonlinearly alters both PAR and canopy temperature. Increasing LAI increases light attenuation through the canopy, which decreases the amount of PAR reaching the lower levels of the canopy and consequently decreases the PAR-dependent emission scaling factor, γ_{PAR}. Using CLM-DP instead of CLM-PRESC increases the standard deviation of canopy temperature (Figure 12), which augments variability of the temperature-dependence emission scaling factor, γ_T. The relationship between variation in LAI and canopy temperature is not straightforward: increasing leaf area increases the latent cooling capacity of the canopy; however, increasing leaf area also increases the canopy radiative absorption capacity. Because the simulated canopy temperature during June, July, and August was, on average, 0.19 K cooler when dynamic phenology was employed than when phenology was prescribed, we surmise that the increased

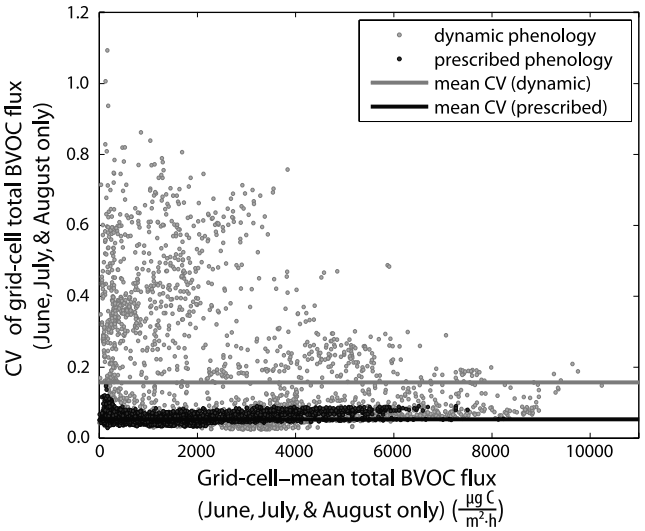

Figure 10. Relation of each grid cell's mean BVOC flux with its coefficient of variation (CV) for 1982–2004. Only BVOC fluxes from June, July, and August are considered in the calculation of mean and CV. CV is the standard deviation divided by the mean.

latent cooling capacity of the canopy is the dominant source of increased variability in canopy temperature and, consequently, in biogenic emissions.

[32] A quantitative assessment of the relative contribution of short-term environmental variation (e.g., shifts of canopy temperature) and the relative contribution of interannual variation in LAI to year-to-year differences in the magnitude of BVOC flux requires parameter substitution experiments within simulations using a coupled land-atmosphere model that allows changes in albedo, transpiration, and surface roughness to feed back to affect regional meteorological conditions. However, we can approximate the relative importance of variation in temperature, radiation, and biomass to the interannual variability of BVOC flux by comparing the component sources of variability from CLM-

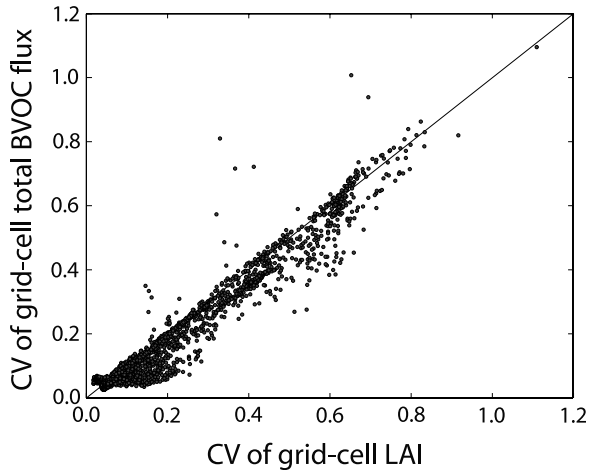

Figure 11. Relation between the coefficient of variation (CV) of leaf area index (LAI) and the CV of BVOC flux. Results are from the simulation that used CLM-DP.

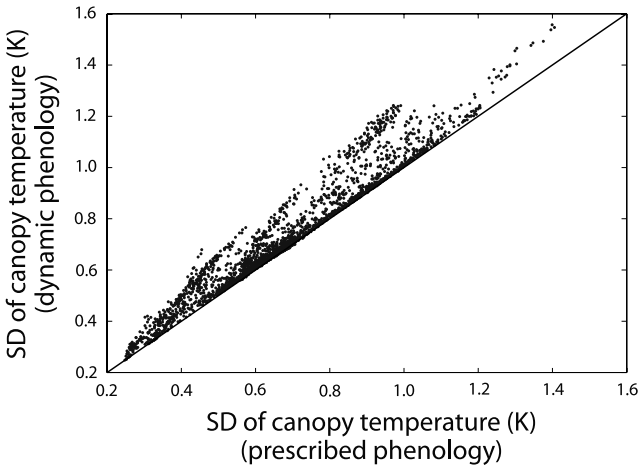

Figure 12. Relation between the standard deviation (SD) of canopy temperature in the CLM-DP run the CLM-PRESC run.

PRESC to those from CLM-DP run. Figure 13 shows the domain-average percent departure from the monthly mean for isoprene and the corresponding domain-average percent departure from the monthly mean for the dimensionless emission-modulating factors γ_{PAR} and γ_T and for LAI. We see in Figure 13 that LAI is a source of variability that is at least of equal importance to PAR and temperature. When seeking accurate assessments of interannual variation in nonisoprene BVOC emissions, which (at least in the model) respond only to variation in temperature, simulating dynamic phenology is at least as important.

[33] Our results, in conjunction with the findings of others [*Levis et al.*, 2003; *Naik et al.*, 2004; *Tao and Jain*, 2005], reinforce the assertion that total biogenic emissions vary significantly between years, by up to a factor of two. Results presented here demonstrate the importance of representing of year-to-year change in leaf biomass density when modeling biogenic emissions and demonstrate the need for improved empirical quantification of interannual variation in leaf biomass density. In Texas, year-to-year variation in precipitation is more important than temperature in controlling the interannual variation of leaf biomass density: our results also provide additional justification for studies that predict future changes to interannual variability of precipitation.

[34] Even small changes in the concentrations of BVOCs can shift the tropospheric ozone production of a region from being NO_x-limited to being VOC-limited, a chemical shift that changes the relative utility of air pollution control policies [*X. M. Wang et al.*, 2005]. For the sake of simplicity, air quality modeling studies often assume that the annual phenological cycle is constant between years and thereby likely underestimate interannual differences in biogenic emissions and air quality.

[35] The preliminary calibration used here provides improved estimates of the magnitude and spatial distribution of year-to-year variation of biogenic emissions in eastern Texas. Such information is immediately useful to Texas air quality managers and policymakers; however, automated multicriteria calibration [e.g., *Bastidas et al.*, 1999] of model parameters will further improve the realism of

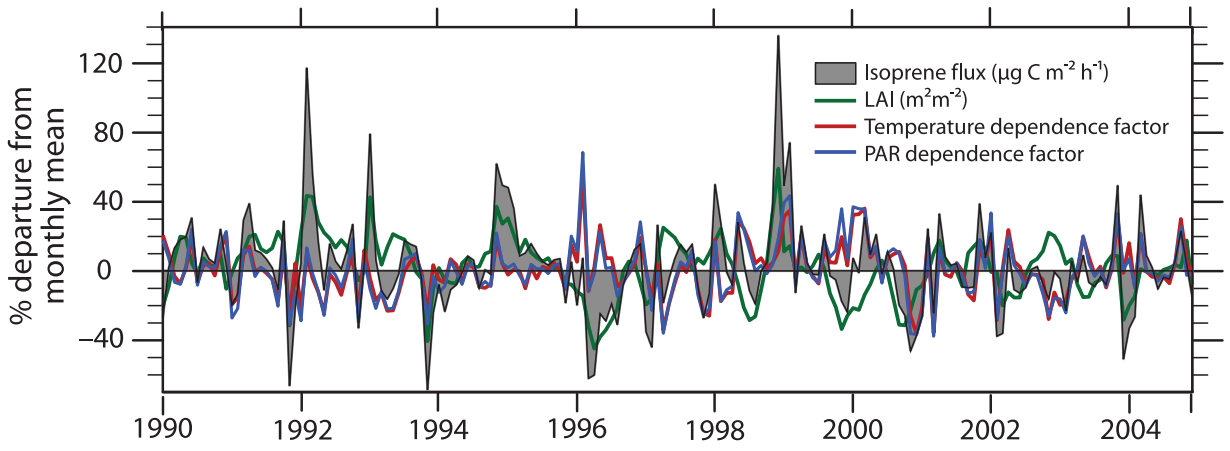

Figure 13. Components of interannual variation in domain-average isoprene emissions (1990–2004). Time series shown are the domain-average% departure from the monthly mean. The temperature dependence factor is γ_T in equation (1). The PAR dependence factor is γ_{PAR} in equation (1). The variability in the time period shown is representative of the variability for the entire simulation period; only years 1990–2004 are shown for ease of viewing.

simulated emissions, will provide uncertainty estimates, and will improve the model's suitability for practical and policy applications.

[36] The biogenic emissions module within CLM depends on the premise that biogenic emissions are a linear function of leaf biomass density. During our preliminary calibration, when we treated the satellite-derived LAI data as truth, we implicitly assumed that leaf biomass density is a linear function of satellite-observed spectral reflectance. The combination of these two assumptions implies that BVOC flux and leaf pigmentation are correlated, which is consistent with empirical studies [*Lehning et al.*, 2001] but which may not be completely accurate.

[37] Our model framework neglects many sources of interannual variation in biogenic emissions. *Geron et al.* [2000] showed that emissions factors for white oak vary seasonally; *Funk et al.* [2003] found evidence for large variation in emission factors over the daily cycle. CLM does not represent the detrimental effect of ozone on plant growth [*Ashmore*, 2005], and it does not account for recent observations showing a decrease in the emission of some chemical species of BVOCs when ambient carbon dioxide concentrations increase [e.g., *Rosenstiel et al.*, 2003]. The BVOC emissions module in CLM does not represent the uptake of atmospheric isoprene from soil microorganisms [*Cleveland and Yavitt*, 1998], the rate of which appears to decrease as soil moisture decreases [*Pegoraro et al.*, 2005]. At least in some plant species, isoprene emissions increase under mild drought stress and then decrease when drought stress becomes severe [*Pegoraro et al.*, 2005; *Funk et al.*, 2005]. In CLM-DP, LAI begins to decrease as soon as photosynthesis falls below the maintenance respiration rate; all else being equal, modeled isoprene flux begins to decrease as soon as maintenance respiration demands more energy than is captured by photosynthesis. CLM-DP therefore likely underestimates BVOC flux in periods of mild water scarcity.

[38] Why go to the effort of augmenting an LSM with a dynamic phenology model when high-resolution satellite-derived observations of LAI are available? Assimilating high-resolution satellite-derived LAI variation is indeed a viable option for retrospective applications. The work of *Guenther et al.* [2006] provides a ready framework for such assimilation. However, such an approach is not amenable to investigation of how future environmental change will alter biomass density and biogenic emissions. Processed-based representations of phenological change also provide a foundation for future assessment of cause-and-effect relationships between BVOCs, leaf biomass density, and other components of the climate system; using prescribed, satellite-derived data would render such investigation impossible.

[39] Realistic modeling of biogenic emissions is fundamentally limited by a dearth of observations. Region-specific biogenic emissions capacities for the coarse-resolution LSM land cover classifications and any estimates in interannual variability of biogenic emissions are, of course, only as good as the species-based information from which they are derived. Although the number of species for which the scientific community has biogenic emissions rate estimates is growing, most plant species have no associated biogenic emissions data and data quantifying intraspecies variation in both type [*Staudt et al.*, 2004] and quantity [e.g., *Funk et al.*, 2005] of biogenic emissions is available for only a very few vegetation species.

4. Summary and Conclusions

[40] We used CLM augmented with a dynamic phenology module, a species-derived land cover data set, and region-specific biogenic emissions factors to estimate the interannual variability of biogenic emissions in eastern Texas for the period 1982–2004.

[41] Using the standard CLM, the domain-mean (domain-maximum) average absolute departure from the monthly mean BVOC flux is 11.7% (70.6%); using CLM with dynamic phenology it is 22.4% (137.7%). The domain-mean (domain-maximum) average absolute departure from the monthly mean flux is lower during summer: it is 15.7% (35.3%) using dynamic phenology; it is 7.0% (23.0%) using prescribed phenology. When phenology is prescribed, the

domain-average coefficient of variation (mean-normalized standard deviation) of the JJA mean BVOC flux is 0.0619. When phenology is allowed to vary with environmental conditions, the domain-average coefficient of variation increases threefold to 0.183.

[42] We conclude that year-to-year variation in leaf biomass density is a significant source of interannual variation in regional biogenic emissions that is at least as important as interannual variation in temperature or photosynthetic active radiation. Phenology-driven biogenic emission variability is greatest in regions with relatively low absolute emissions: as a grid cell's mean BVOC flux increases, the mean-normalized standard deviation of mean BVOC flux tends to decrease. Variability is highest in subhumid, sparsely wooded regions where interannual variability of precipitation is relatively large.

[43] Our model framework lays the groundwork for future coupled climate model investigations of the cause-and-effect relationships between biogenic emissions, other land surface states and fluxes, and atmospheric processes. Our results are for Texas, but the presented results likely apply elsewhere.

Appendix A

[44] We define the absolute percent departure from the mean for a time series x as follows:

$$\forall x_{y,m}; y = y_s, y_{s+1}, \ldots, y_e; m = 1, 2, \ldots, 12$$

$$\overline{x_m} = \frac{\sum_{y=y_s}^{y_e} x_{y,m}}{(y_e - y_s + 1)} \tag{A1}$$

$$d_{y,m} = \left| \frac{x_{y,m} - \overline{x_m}}{\overline{x_m}} \right| \tag{A2}$$

$$\overline{d_{m_s - m_e}} = \frac{\sum_{y=y_s}^{y_e} \sum_{m=m_s}^{m_e} d_{y,m}}{(y_e - y_s + 1) \times (m_e - m_s + 1)} \tag{A3}$$

$$\max(d_{m_s - m_e}) = \max\left(d_{y,m}\right), y = y_s, y_{s+1}, \ldots, y_e, \quad m = m_s, m_{s+1}, \ldots, m_e \tag{A4}$$

Where $x_{y,m}$ is a member of time series x. $x_{y,m}$ is the monthly mean value of the variable of interest for month m of year y (equation (A1)). The first and last years of time series x are y_s and y_e (1982 and 2004, in the results described in this paper). For a given month m in year y, that month's absolute departure from the monthly mean is $d_{y,m}$ (equation (A2)). The average absolute departure from the monthly mean for the time series x considering only the set of months that begins with m_s and ends with m_e is $\overline{d_{m_s - m_e}}$(equation (A3)). The maximum absolute departure from the monthly mean for the time series considering only the set of months that begins with m_s and ends with m_e is max ($d_{m_s} - m_e$) (equation (A4)). To compute the domain-mean (domain-maximum) average absolute departure from the mean, we first calculated the average absolute departure from the mean for each grid cell and then calculated the mean (maximum) of the values for all grid cells that compose the domain.

[45] **Acknowledgments.** We are particularly grateful to Peter Lawrence, who provided us with the satellite-derived land cover data set and who lent us many useful insights. We are also grateful for the constructive comments of three anonymous reviewers, David Allen, Mark Estes, Enrique Rosero, Xiaoyan Jiang, Xuemei Wang, Robert Dickinson, and Hua Su. This work was funded by the U.S. Environmental Protection Agency's Science to Achieve Results (STAR) program grant RD83145201. Thanks to the Texas Advanced Computing Center for providing computing resources.

References

Andreae, M. O., and P. J. Crutzen (1997), Atmospheric aerosols: Biogeochemical sources and role in atmospheric chemistry, *Science*, *276*, 1052–1058.

Ashmore, M. R. (2005), Assessing the future global impacts of ozone on vegetation, *Plant Cell Environ.*, *28*, 949–964.

Bastidas, L. A., H. V. Gupta, S. Sorooshian, W. J. Shuttleworth, and Z. L. Yang (1999), Sensitivity analysis of a land surface scheme using multicriteria methods, *J. Geophys. Res.*, *104*(D16), 19,481–19,490.

Bonan, G. B. (1996), A land surface model (LSM version 1.0) for ecological, hydrological, and atmospheric studies: Technical description and user's guide, *NCAR Tech. Note, NCAR/TN-417+STR,* Natl. Cent. for Atmos. Res., Boulder, Colo.

Bonan, G. B., and S. Levis (2006), Evaluating aspects of the community land and atmosphere models (CLM3 and CAM3) using a dynamic global vegetation model, *J. Clim.*, *19*, 2290–2301.

Bonan, G. B., S. Levis, L. Kergoat, and K. W. Oleson (2002a), Landscapes as patches of plant functional types: An integrating concept for climate and ecosystem models, *Global Biogeochem. Cycles*, *16*(2), 1021, doi:10.1029/2000GB001360.

Bonan, G. B., K. W. Oleson, M. Vertenstein, S. Levis, X. B. Zeng, Y. J. Dai, R. E. Dickinson, and Z. L. Yang (2002b), The land surface climatology of the community land model coupled to the NCAR community climate model, *J. Clim.*, *15*, 3123–3149.

Chameides, W. L., et al. (1988), The role of biogenic hydrocarbons in urban photochemical smog—Atlanta as a case-study, *Science*, *241*, 1473–1475.

Claeys, M., et al. (2004), Formation of secondary organic aerosols through photooxidation of isoprene, *Science*, *303*, 1173–1176.

Cleveland, C. C., and J. B. Yavitt (1998), Microbial consumption of atmospheric isoprene in a temperate forest soil, *Appl. Environ. Microbiol.*, *64*, 172–177.

Collatz, G. J., C. Grivet, J. T. Ball, and J. A. Berry (1991), Physiological and environmental-regulation of stomatal conductance, photosynthesis, and transpiration - A model that includes a laminar boundary-layer, *Agric. For. Meteorol.*, *54*, 107–136.

Collatz, G. J., M. Ribas-Carbo, and J. A. Berry (1992), Coupled photosynthesis-stomatal conductance model for leaves of C4 plants, *Aust. J. Plant Physiol.*, *19*, 519–538.

Dickinson, R. E. (1983), Land surface processes and climate—Surface albedos and energy balance, *Adv. Geophys.*, *25*, 305–353.

Dickinson, R. E., M. Shaikh, R. Bryant, and L. Graumlich (1998), Interactive canopies for a climate model, *J. Clim.*, *11*, 2823–2836.

Dougherty, R. L., J. A. Bradford, P. I. Coyne, and P. L. Sims (1994), Applying an empirical model of stomatal conductance to three C-4 grasses, *Agric. For. Meteorol.*, *67*, 269–290.

Farquhar, G. D., S. von Caemmerer, and J. A. Berry (1980), A biochemical model of photosynthetic CO_2 assimilation in leaves of C species, *Planta*, *149*, 78–90.

Fuentes, J. D., and D. Wang (1999), On the seasonality of isoprene emissions from a mixed temperate forest, *Ecol. Appl.*, *9*, 1118–1131.

Fuentes, J. D., D. Wang, H. H. den Hartog, H. H. Neumann, T. F. Dann, and K. J. Puckett (1995), Modelled and field-measurements of biogenic hydrocarbon emissions from a Canadian deciduous forest, *Atmos. Environ.*, *29*, 3003–3017.

Funk, J. L., C. G. Jones, C. J. Baker, H. M. Fuller, C. P. Giardina, and M. T. Lerdua (2003), Diurnal variation in the basal emission rate of isoprene, *Ecol. Appl.*, *13*, 269–278.

Funk, J. L., C. G. Jones, D. W. Gray, H. L. Throop, L. A. Hyatt, and M. T. Lerdau (2005), Variation in isoprene emission from Quercus rubra: Sources, causes, and consequences for estimating fluxes, *J. Geophys. Res.*, *110*, D04301, doi:10.1029/2004JD005229.

Geron, C., et al. (2000), Temporal variability in the basal isoprene emission factor, *Tree Physiol.*, *20*, 799–805.
Gholz, H. L. (1982), Environmental limits on above-ground net primary production, leaf-area, and biomass in vegetation zones of the Pacific Northwest, *Ecology*, *63*, 469–481.
Grier, C. C., and S. W. Running (1977), Leaf area of mature northwestern coniferous forests—Relation to site water-balance, *Ecology*, *58*, 893–899.
Guenther, A. (1997), Seasonal and spatial variations in natural volatile organic compound emissions, *Ecol. Appl.*, *7*, 34–45.
Guenther, A. (2002), The contribution of reactive carbon emissions from vegetation to the carbon balance of terrestrial ecosystems, *Chemosphere*, *49*, 837–844.
Guenther, A., R. K. Monson, and R. Fall (1991), Isoprene and monoterpene emission rate variability: Observations with eucalyptus and emission rate algorithm development, *J. Geophys. Res.*, *96*(D6), 10,799–10,808.
Guenther, A., et al. (1995), A global model of natural volatile organic compound emissions, *J. Geophys. Res.*, *100*(D5), 8873–8892.
Guenther, A., T. Karl, P. Harley, C. Wiedinmyer, P. I. Palmer, and C. Geron (2006), Estimates of global terrestrial isoprene emissions using MEGAN (Model of Emissions of Gases and Aerosols from Nature), *Atmos. Chem. Phys.*, *6*, 3181–3210.
Gulden, L. E., and Z. L. Yang (2006), Development of species-based, regional emission capacities for simulation of biogenic volatile organic compound emissions in land-surface models: An example from Texas, USA, *Atmos. Environ.*, *40*, 1464–1479.
Kavouras, I. G., N. Mihalopoulos, and E. G. Stephanou (1998), Formation of atmospheric particles from organic acids produced by forests, *Nature*, *395*, 683–686.
Kim, Y., and G. L. Wang (2005), Modeling seasonal vegetation variation and its validation against Moderate Resolution Imaging Spectroradiometer (MODIS) observations over North America, *J. Geophys. Res.*, *110*, D04106, doi:10.1029/2004JD005436.
Kucharik, C. J., et al. (2006), A multiyear evaluation of a dynamic global vegetation model at three AmeriFlux forest sites: Vegetation structure, phenology, soil temperature, and CO_2 and H_2O vapor exchange, *Ecol. Modell.*, *196*, 1–31.
Lathière, J., D. A. Hauglustaine, N. De Noblet-Ducoudré, G. Krinner, and G. A. Folberth (2005), Past and future changes in biogenic volatile organic compound emissions simulated with a global dynamic vegetation model, *Geophys. Res. Lett.*, *32*, L20818, doi:10.1029/2005GL024164.
Lawrence, P. J., and T. N. Chase (2007), Representing a new MODIS consistent land surface in the Community Land Model (CLM 3.0), *J. Geophys. Res.*, *112*, G01023, doi:10.1029/2006JG000168.
Lehning, A., W. Zimmer, I. Zimmer, and J.-P. Schnitzler (2001), Modeling of annual variations of oak (*Quercus robur* L.) isoprene synthase activity to predict isoprene emission rates, *J. Geophys. Res.*, *106*(D3), 3157–3166.
Leuschner, C., et al. (2006), Variation in leaf area index and stand leaf mass of European beech across gradients of soil acidity and precipitation, *Plant Ecol.*, *186*, 247–258.
Levis, S., C. Wiedinmyer, G. B. Bonan, and A. Guenther (2003), Simulating biogenic volatile organic compound emissions in the community climate system model, *J. Geophys. Res.*, *108*(D21), 4659, doi:10.1029/2002JD003203.
Levis, S., G. B. Bonan, M. Vertenstein, and K. W. Oleson (2004), The Community Land Model's dynamic global vegetation model (CLM-DGVM): Technical description and user's guide, *NCAR Tech. Note TN-459+IA*, 50 pp., Natl. Center for Atmos. Res., Boulder, Colo.
Mesinger, F., et al. (2006), North American regional reanalysis, *Bull. Am. Meteorol. Soc.*, *87*, 343–360.
Monson, R. K., et al. (1994), Environmental and developmental controls over the seasonal pattern of isoprene emission from aspen leaves, *Oecologia*, *99*, 260–270.
Naik, V., C. Delire, and D. J. Wuebbles (2004), Sensitivity of global biogenic isoprenoid emissions to climate variability and atmospheric CO_2, *J. Geophys. Res.*, *109*, D06301, doi:10.1029/2003JD004236.
Novakov, T., and J. E. Penner (1993), Large contribution of organic aerosols to cloud-condensation-nuclei concentrations, *Nature*, *365*, 823–826.
Oleson, K. W. et al. (2004), Technical description of the Community Land Model, *NCAR Tech. Note TN-461+STR*, 174 pp., Natl. Center for Atmos. Res., Boulder, Colo.
Palmer, P. I., et al. (2006), Quantifying the seasonal and interannual variability of North American isoprene emissions using satellite observations of the formaldehyde column, *J. Geophys. Res.*, *111*, D12315, doi:10.1029/2005JD006689.
Pegoraro, E., et al. (2005), The effect of elevated atmospheric CO_2 and drought on sources and sinks of isoprene in a temperate and tropical rainforest mesocosm, *Global Change Biol.*, *11*(8), 1234–1246.
Poisson, N., et al. (2000), Impact of non-methane hydrocarbons on tropospheric chemistry and the oxidizing power of the global troposphere: 3-dimensional modelling results, *J. Atmos. Chem.*, *36*, 157–230.
Possell, M., et al. (2004), Interactive effects of elevated CO_2 and soil fertility on isoprene emissions from Quercus robur, *Global Change Biol.*, *10*(11), 1835–1843.
Rosenstiel, T. N., et al. (2003), Increased CO_2 uncouples growth from isoprene emission in an agriforest ecosystem, *Nature*, *421*, 256–259.
Sellers, P. J. (1985), Canopy reflectance, photosynthesis and transpiration, *Int. J. Remote Sens.*, *6*, 1335–1372.
Simpson, D., et al. (1999), Inventorying emissions from nature in Europe, *J. Geophys. Res*, *104*(D7), 8113–8152.
Smiatek, G., and M. Bogacki (2005), Uncertainty assessment of potential biogenic volatile organic compound emissions from forests with the Monte Carlo method: Case study for an episode from 1 to 10 July 2000 in Poland, *J. Geophys. Res.*, *110*, D23304, doi:10.1029/2004JD005685.
Staudt, M., C. Mir, R. Joffre, S. Rambal, A. Bonin, D. Landais, and R. Lumaret (2004), Isoprenoid emissions of *Quercus* spp. (*Q. suber* and *Q. ilex*) in mixed stands contrasting in interspecific genetic introgression, *New Phytol.*, *163*, 573–584.
Tao, Z. N., and A. K. Jain (2005), Modeling of global biogenic emissions for key indirect greenhouse gases and their response to atmospheric CO_2 increases and changes in land cover and climate, *J. Geophys. Res.*, *110*, D21309, doi:10.1029/2005JD005874.
Tian, Y., R. E. Dickinson, L. Zhou, and M. Shaikh (2004), Impact of new land boundary conditions from Moderate Resolution Imaging Spectroradiometer (MODIS) data on the climatology of land surface variables, *J. Geophys. Res.*, *109*, D20115, doi:10.1029/2003JD004499.
Wang, K. Y., and D. E. Shallcross (2000), Modelling terrestrial biogenic isoprene fluxes and their potential impact on global chemical species using a coupled LSM-CTM model, *Atmos. Environ.*, *34*, 2909–2925.
Wang, Q., et al. (2005), On the relationship of NDVI with leaf area index in a deciduous forest site, *Remote Sens. Environ.*, *94*, 244–255.
Wang, X. M., G. Carmichael, D. L. Chen, Y. H. Tang, and T. J. Wang (2005), Impacts of different emission sources on air quality during March 2001 in the Pearl River Delta (PRD) region, *Atmos. Environ.*, *39*, 5227–5241.
Wiedinmyer, C., A. Guenther, M. Estes, I. W. Strange, G. Yarwood, and D. T. Allen (2001), A land use database and examples of biogenic isoprene emission estimates for the state of Texas, USA, *Atmos. Environ.*, *35*, 6465–6477.

L. E. Gulden, G.-Y. Niu, and Z.-L. Yang, Department of Geological Sciences, John A. and Katherine G. Jackson School of Geosciences, 1 University Station C1100, University of Texas at Austin, Austin, TX 78712-0254, USA. (liang@mail.utexas.edu)